

## Effect of Protein, Polysaccharide, and Oxygen Concentration Profiles on Biofilm Cohesiveness<sup>∇</sup>

Francois Ahimou,<sup>1\*</sup> Michael J. Semmens,<sup>2</sup> Greg Haugstad,<sup>3</sup> and Paige J. Novak<sup>2</sup>

3M Medical Division, Saint Paul, Minnesota 55144,<sup>1</sup> and Department of Civil Engineering<sup>2</sup> and Characterization Facility,<sup>3</sup> University of Minnesota, Minneapolis, Minnesota 55455

Received 14 October 2006/Accepted 17 February 2007

**It is important to control biofilm cohesiveness to optimize process performance. In this study, a membrane-aerated biofilm reactor inoculated with activated sludge was used to grow mixed-culture biofilms of different ages and thicknesses. The cohesions, or cohesive energy levels per unit volume of biofilm, based on a reproducible method using atomic force microscopy (F. Ahimou, M. J. Semmens, P. J. Novak, and G. Haugstad, *Appl. Environ. Microbiol.* 73:2897–2904, 2007), were determined at different locations within the depths of the biofilms. In addition, the protein and polysaccharide concentrations within the biofilm depths, as well as the dissolved oxygen (DO) concentration profiles within the biofilms, were measured. It was found that biofilm cohesion increased with depth but not with age. Level of biofilm cohesive energy per unit volume was strongly correlated with biofilm polysaccharide concentration, which increased with depth in the membrane-aerated biofilm. In a 12-day-old biofilm, DO also increased with depth and may therefore be linked to polysaccharide production. In contrast, protein concentration was relatively constant within the biofilm and did not appear to influence cohesion.**

Biofilms are ubiquitous in nature, and they can be beneficial or troublesome, depending upon where and how they grow. There appears to be a consensus that the content of extracellular polymeric substances (EPS) is important in biofilm cohesion and biofilm adhesion to surfaces. For example, Klapper et al. (17) used a model based on polymer viscoelastic properties and suggested that the material properties of biofilm were largely determined by the EPS, implying that biofilm strength should indeed be linked to EPS quantity and composition. In addition, a recent study by Xavier et al. (35) proposed a kinetic model to describe biofilm detachment that was based on enzymatic disruption of the EPS matrix, thereby affecting biofilm cohesiveness.

The EPS content of a biofilm can differ in quantity and character as a result of environmental factors. Numerous environmental factors have been reported to promote EPS production. These include high levels of oxygen (4), limited availability of nitrogen (15, 22), desiccation (25), low temperature (16), low pH (28), and nutrient deprivation (20). Weiner et al. (34) described several roles and functions for EPS, including that of protection against environmental stress. In addition, Davies et al. (8) showed that activation of a gene (*algC*) for production of the exopolymer alginate was higher for *Pseudomonas aeruginosa* when attached to a Teflon mesh than for unattached *P. aeruginosa*. This suggests that organisms are able to respond to their environments and change EPS compositions and therefore their adhesion abilities, based on the surfaces to which they attach. Multivalent cations, such as those of calcium and magnesium, also probably play a role in the cohesiveness of microbial aggregates, as evaluated from studies

of anaerobic sludge granules (12), activated sludge flocs (13), and biofilms (6), by bridging negatively charged sites on extracellular polymers to create stable intermolecular and cell-EPS connections (21).

Despite research on EPS and, in particular, EPS involvement in microbial surface interactions, the precise role of EPS in biofilm cohesiveness is not completely understood and the literature is contradictory on this matter. For example, Applegate and Bryers (3) attributed the susceptibility to sloughing observed in oxygen-limited biofilms to the higher EPS production under these conditions, while Ohashi and Harada (23) found that biofilm adhesion strength was not dependent on the quantity of EPS present.

So far, very limited studies regarding the cohesive strength levels of biofilms and how strength changes within a biofilm have been performed. Biofilms are highly stratified and characterized by a heterogeneous structure, not only in the composition and the distribution of EPS but also by defined aerobic/anoxic zones within the biofilm depth (5). This can affect microbial growth rate and, potentially, EPS production (33). The relationships between biofilm cohesiveness and properties such as EPS composition and distribution across the biofilm depth, although important for understanding, predicting, and controlling biofilm adhesion and sloughing, remain unknown.

In this paper, we extracted and determined polysaccharide and protein concentrations from various depths in biofilms of different ages. The effect of these two EPS components on the level of cohesive energy per unit volume of biofilm, a surrogate for strength, was investigated across biofilm depth using atomic force microscopy (AFM) (1). These results improve our understanding of biofilm cohesion and should help us design new strategies for controlling biofilm development, such as techniques focused on weakening certain portions of the EPS or controlling the oxidation states of biofilms for better cohesion.

\* Corresponding author. Mailing address: 3M Medical Division, 3M Center, Building 270-03-N-02, Saint Paul, MN 55144. Phone: (651) 737-3436. Fax: (651) 737-2660. E-mail: fahimou@mmm.com.

<sup>∇</sup> Published ahead of print on 2 March 2007.

## MATERIALS AND METHODS

**Membrane-aerated biofilm reactor.** Biofilms were grown from activated sludge containing a diverse community of bacteria as previously described (1). Multiple membrane test modules were submerged at the same time in the reactor to support the growth of the biofilms over a 12-day period. Biofilms grown on membranes without added air were used as controls. Membranes were removed from the bioreactor on different days to assess the impact of age on biofilm properties.

**DO profile determination.** Dissolved oxygen (DO) profiles across the biofilm were obtained using a Clark-type microelectrode (model OS-10; Unisense, Aarhus, Denmark). This microelectrode had a 10- to 15- $\mu\text{m}$  tip diameter, a rapid response time ( $<5$  s), and a spatial resolution of 20 to 30  $\mu\text{m}$ . The biofilm-covered membrane was mounted horizontally, and the microelectrode was lowered into the biofilm by using a computer-controlled micromanipulator (Oriel Inst., Stratford, CT) capable of advancing in 0.1- $\mu\text{m}$  increments. The surface of the membrane was detected when the DO concentration reached the saturation DO concentration at the membrane surface (31). The DO profile was captured on a computer using Profix 2.1 software.

**Biofilm thickness measurement.** Biofilm thickness was measured optically using a traveling micromanipulator microscope (Integrated Endoscopy, Irvine, CA) that could be moved in the  $x$ ,  $y$ , and  $z$  directions. The microscope was first focused at a fixed reference surface (such as a point on the stainless steel manifold), and the height ( $h_A$ ) was measured. The microscope was then focused on the top surface of the biofilm, and the corresponding distance ( $h_B$ ) was read. Finally, the microscope was focused on the membrane support surface (the bottom of the biofilm) and the value ( $h_C$ ) was also read. The two distances traveled by the micromanipulator were determined, and the thicknesses of the biofilms were obtained by subtraction  $[(h_C - h_A) - (h_B - h_A)]$  as described by Cole et al. (7). The thicknesses of the biofilms were averaged from six independent measurements.

**Protein and polysaccharide extraction and quantification.** Biofilms grown over a 12-day period were removed from the bioreactor and sectioned in 200- $\mu\text{m}$  slices (parallel to the membrane surface) using a combined cryostat-microtome apparatus (Richard-Allan Scientific, Kalamazoo, MI). Each biofilm section was transferred to a sterile microcentrifuge tube and stored separately at  $-20^\circ\text{C}$  until use. Biofilm samples (1.5 g) from the same age and depth groups were weighed and split equally into three separate tubes (0.5 g/tube) for dry weight (overnight at  $103^\circ\text{C}$ ), protein, and polysaccharide quantification. For protein and polysaccharide quantification, the samples were first dried by vacuum centrifugation (Labnet, Edison, NJ), resuspended in 1 N NaOH, and heated at  $80^\circ\text{C}$  for 30 min in a water bath. The samples were then centrifuged at 10,000 rpm and  $4^\circ\text{C}$  for 15 min. The supernatants were collected for protein and polysaccharide quantification.

The protein content was measured using a method modified from that of Lowry et al. (19) as described by Raunkjær et al. (27). The method described by Lowry et al. was followed, except that  $\text{CuSO}_4 \cdot 5\text{H}_2\text{O}$  and sodium tartrate solutions were prepared and kept separately until the day of analysis to prevent precipitation in the mixture. Bovine serum albumin was used as a standard. The absorbance was measured at 750 nm.

The polysaccharide content was measured using the anthrone method (10) as modified by Raunkjær et al. (27) to eliminate the effect of a non-anthrone-specific color development. A correction was made by subtracting the background color without addition of the anthrone reagent; this was typically 10% of the sample values. Glucose was used as a standard, and the absorbance was measured at 625 nm. This provides an estimation of the concentration of hexose sugars in a sample.

**Biofilm preparation and imaging.** Membrane modules were removed from the bioreactor after each test period, and the biofilm was excavated from the top using a scalpel and a  $\times 250$ -magnification microscope (Integrated Endoscopy, Irvine, CA). Surface layers were removed until a desired biofilm thickness was obtained. The AFM method for scanning the biofilm, measuring the volume of displaced biofilm, and determining the friction force is described elsewhere, as is the method for calculating the level of cohesive energy per unit volume of biofilm (1). Briefly, a wet piece ( $\sim 1$  by 1 cm) of the membrane and attached biofilm was cut and placed into a chamber ( $\sim 90\%$  humidity level) containing a saturated NaCl solution/excess salt at room temperature. After equilibration (1 hour), these biofilm-coated membrane samples were mounted on the AFM (PicoSPM; Molecular Imaging) apparatus for scanning at a constant humidity (M scanner [lateral range = 30  $\mu\text{m}$ ; vertical range = 7  $\mu\text{m}$ ]). The consecutive, nonperturbative 5- by 5- $\mu\text{m}$  height images, each following four raster abrasions, were subtracted to obtain the volume of displaced biofilm. The friction force was quantified from histograms of friction difference images, i.e., the number of

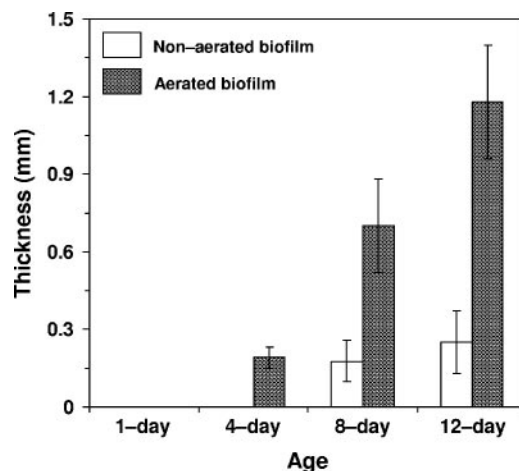


FIG. 1. Effect of aeration and age on biofilm thickness. Error bars represent the standard deviations of the means ( $n = 6$ ).

image pixels within incremental friction force intervals. The corresponding frictional-energy dissipation was summed from each set of four consecutive raster scans and normalized by the volume of material displaced to obtain the level of biofilm cohesive energy per unit volume.

## RESULTS

As expected, the biofilm thickness increased with age over the 12-day test period, as shown in Fig. 1. Under aerated conditions, a thin visible biofilm layer appeared after 1 day, compared to 4 days under nonaerated conditions. After the 12-day test period, the aerated biofilm was four times thicker than the biofilm grown on the membrane support to which no air was supplied.

The biofilms were excavated as described above and imaged by AFM. Figures 2 and 3 show the AFM topographic images at the tops of the biofilm layers before (Fig. 2) and after (Fig. 3) abrasion with an elevated load (40 nN). The volume of biofilm displaced after the same number of raster scans at a given load was greater at the top of the biofilm and decreased with depth, regardless of biofilm age. This suggests that the cohesive properties of the biofilm were not significantly affected by excavating the biofilm with the scalpel, for if the technique had modified the biofilm properties, similar abrasion responses from each of the slice faces (regardless of the original depth in the biofilm) should have been observed. Cohesive energy levels are shown versus depth in Fig. 4 for biofilms of different ages. These results indicate that under aeration, the cohesion, or level of cohesive energy per unit volume, increased with depth. In addition, at a given biofilm depth, no significant difference in cohesion was found when biofilms of different ages were compared. Biofilms grown without aeration were weak and sloughing easily. Therefore, we were unable to measure the cohesive energy levels for the 8- and 12-day-old nonaerated biofilms. The lowest cohesion was obtained when the biofilm was not aerated. This shows that the cohesion, or level of cohesive energy per unit volume, is strongly dependent on biofilm depth and not on biofilm age and is also strongly influenced by aeration.

Polysaccharide and protein were extracted from biofilm slices, and their concentrations were determined as a function

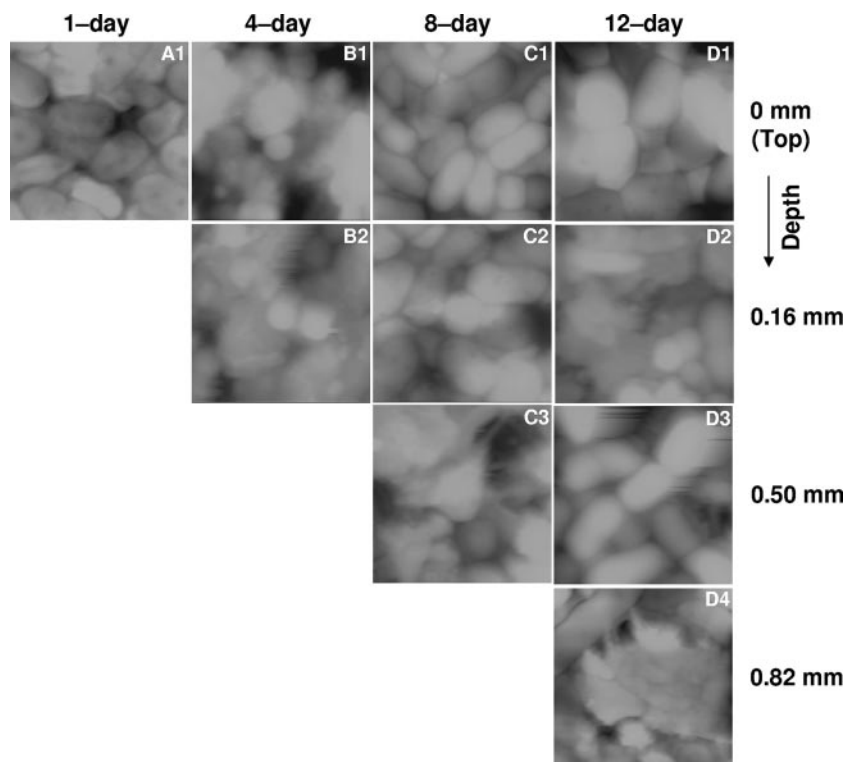


FIG. 2. Topographic images ( $5 \text{ by } 5 \mu\text{m}$ ; contrast range,  $0.8 \text{ to } 2 \mu\text{m}$ ) of nonabraded biofilms used as controls in cohesive energy calculation. Images were collected from left to right (trace) at an  $\sim 0\text{-nN}$  applied load.

of biofilm depth and age (Table 1). Polysaccharide concentration increased with depth but not with biofilm age. Protein concentration, in contrast, was relatively constant regardless of biofilm depth or age. The lowest polysaccharide and protein concentrations were obtained when the biofilm was not aerated. Figure 5 shows the level of biofilm cohesive energy per unit volume as a function of the polysaccharide and protein concentrations and their sums and ratios. It is evident that the level of cohesive energy per unit of biofilm volume correlates well with both the polysaccharide concentration ( $R = 0.90$ ) and the polysaccharide to protein ratio ( $R = 0.92$ ). In contrast, the correlation with protein concentration is poor ( $R = 0.59$ ).

The DO concentration was determined across the depth of the 12-day biofilm, and the results are presented in Fig. 6. In this case, the biofilm was 1 mm thick. A depth of 1 mm therefore represents the membrane surface. The base of the biofilm in contact with the membrane surface was in equilibrium with the air supplied to the membrane and was therefore saturated with DO. The DO declined rapidly within the biofilm so that only the bottom 100 to 120  $\mu\text{m}$  of the biofilm was aerobic, with the remainder of the biofilm anaerobic.

## DISCUSSION

Biofilm detachment is one of the critical factors that balance growth and plays a role in controlling the thicknesses of biofilms. Recent attempts to mathematically elucidate the mechanism of biofilm detachment have highlighted the need to measure biofilm cohesiveness (26). To our knowledge, there are no reports available in the literature that present experi-

mental data related to the level of cohesive energy per unit volume across the depth of a biofilm. Here, we found that cohesion is variable within a single membrane-aerated biofilm and increases with the biofilm depth and polysaccharide content of the EPS (Fig. 4 and 5).

The existing literature on biofilm density, EPS, and cohesion cannot point to clear relationships between these properties. Several investigators have profiled the depth dependence of biofilm density and shown that biofilm density increases with depth (5, 36). There is, however, no good reason to believe that density and the cohesive properties of a biofilm are related. Indeed, Ohashi et al. (24) found that biofilm tensile strength was not well correlated with biofilm density. In addition, information on the role of EPS in biofilm cohesiveness is limited and contradictory. Some reports indicate that EPS content is not associated with biofilm adhesion strength (23), while others emphasize the influence of EPS on both the structures and the strength levels of biofilms (2, 9). These conflicting results may be explained by the complexity of EPS, because it contains proteins, polysaccharides, nucleic acids, and lipids, each of which may differ in concentration and structure in biofilms grown under different conditions, and each of which may affect strength and cohesive/adhesive properties differently. In fact, the role of specific EPS components in biofilm structure and cohesion has not been clearly elucidated. Gehrke et al. (11) reported that the lipopolysaccharide fraction of EPS appears to be involved in attachment to solid substrates, such as pyrite and sulfur. Hughes et al. (14) suggested that the disruption of *Enterobacter agglomerans* biofilm by the bacteriophage SF153b

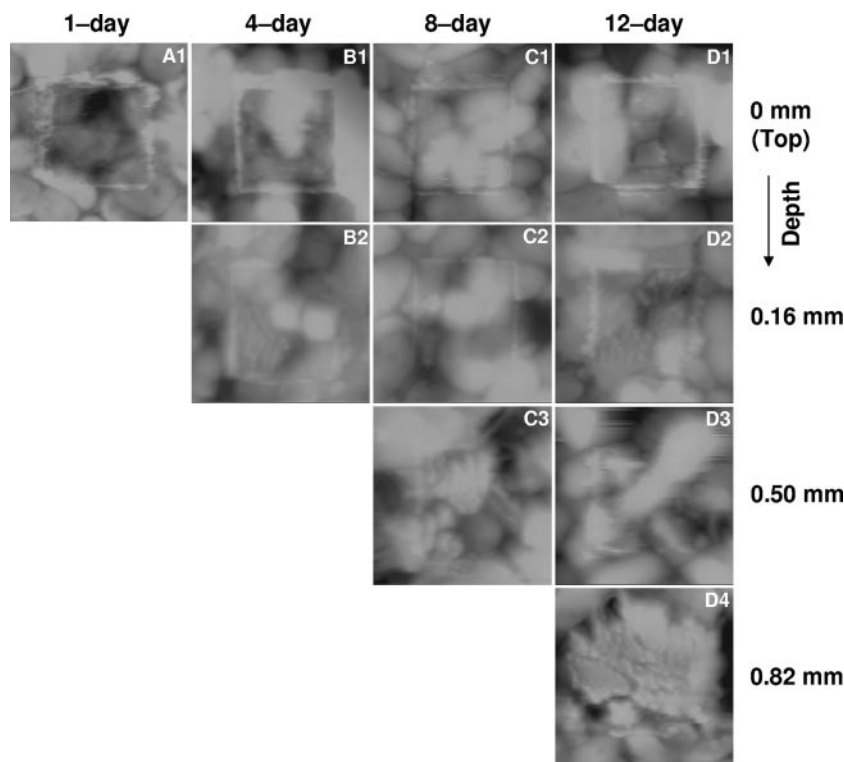


FIG. 3. Topographic images ( $5$  by  $5$   $\mu\text{m}$ ; contrast range,  $0.8$  to  $2$   $\mu\text{m}$ ) exhibiting a  $2.5$ - by  $2.5$ - $\mu\text{m}$  abraded biofilm region. Images were collected from left to right (trace) at an  $\sim 0$ -nN applied load force.

was a combination of EPS degradation by a specific polysaccharide depolymerase enzyme and a subsequent cell lysis.

Our results show that the EPS concentration profile, in terms of protein plus polysaccharide, is correlated with the cohesive energy profile of a membrane-aerated biofilm ( $R = 0.78$ ), which is consistent with previous reports that found that

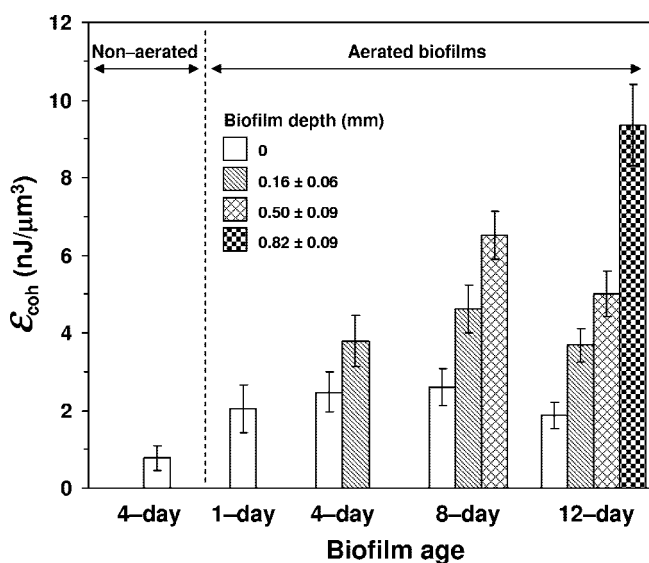


FIG. 4. Biofilm cohesive energy as a function of biofilm age and depth. Error bars represent the standard deviations of the means ( $n = 4$ ).  $\epsilon_{\text{coh}}$ , cohesive energy value.

EPS affected biofilm cohesion (2, 33). Among the two main components of EPS, polysaccharides appeared to strongly affect the level of cohesive energy per unit volume of biofilm ( $R = 0.90$ ). To our knowledge, this is the first report in the literature on the protein and polysaccharide concentration profiles within a biofilm and the corresponding cohesive energy profile across the depth of the same biofilm. Our results suggest that the polysaccharide content of EPS and the environmental factors that influence the polysaccharide content of a biofilm play a key role in biofilm cohesion.

Several factors, such as high levels of oxygen, have been reported to trigger the production of polysaccharides (4). We found that polysaccharide concentration, rather than bulk EPS concentration, followed the same general trend as DO concen-

TABLE 1. EPS composition as a function of biofilm age and depth

Condition	Biofilm age (days)	Biofilm depth (mm)	Concn <sup>a</sup> (mg/g dry wt) for:	
			Polysaccharides	Proteins
Aerated biofilms	1	<0.2	$5 \pm 2$	$58 \pm 7$
	8	0.2	$27 \pm 7$	$210 \pm 12$
	8	0.4	$78 \pm 8$	$221 \pm 8$
	8	0.6	$94 \pm 8$	$193 \pm 13$
	12	0.2	$15 \pm 5$	$133 \pm 11$
	12	0.4	$12 \pm 3$	$79 \pm 9$
	12	0.6	$38 \pm 6$	$131 \pm 12$
	12	0.8	$86 \pm 11$	$119 \pm 9$
Nonaerated biofilms	4	<0.2	$1.3 \pm 0.6$	$14 \pm 5$

<sup>a</sup> Standard deviations were obtained from three separate biofilms.

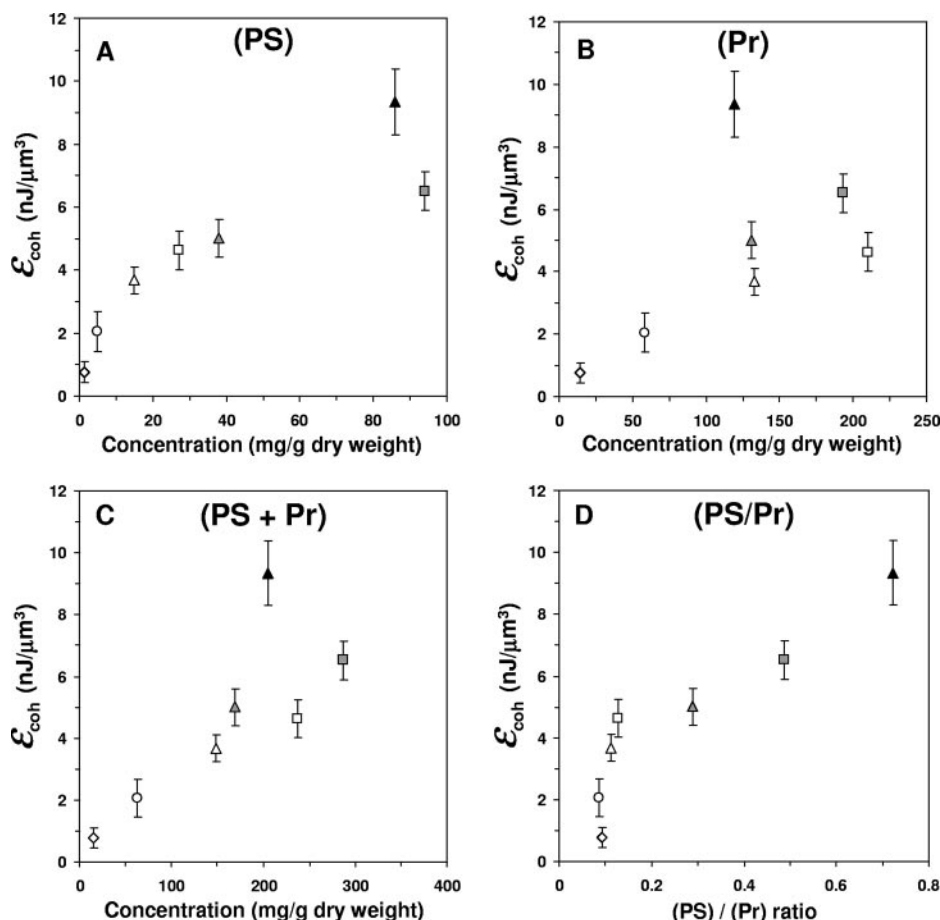


FIG. 5. Relation between cohesive energy and the concentration profiles of polysaccharides (PS) (A), proteins (Pr) (B), their sums (C), and their ratios (D), plotted at given biofilm ages (circle symbols, 1 day; square symbols, 8 days; triangle symbols, 12 days) and depths (open symbols,  $\leq 0.2$  mm; gray symbols, 0.6 mm; closed symbols, 0.8 mm). Error bars represent the standard deviations of the means ( $n = 4$ ).  $\epsilon_{coh}$ , cohesive energy value.

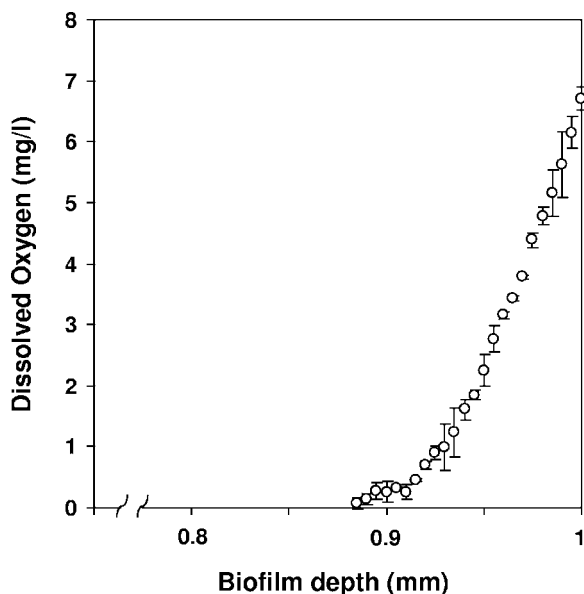


FIG. 6. Measured DO concentration profile of an air-fed, 12-day-old biofilm. The biofilm was  $\sim 1$  mm thick, so a depth of 1.0 mm corresponds to the membrane surface. Error bars represent the standard deviations of the means ( $n = 2$ ).

tration within our biofilms. The observation that the polysaccharide and DO concentrations follow similar profiles is in agreement with the conclusions of Tay et al. (32). They reported that polysaccharide content increased with aeration rates (32). Other researchers, however, have investigated less specific effects of oxygen, such as its effect on biofilm density or bulk EPS production, and observed conflicting results. For example, Lapidou and Rittmann (18) modeled the density development of biofilms and suggested that low oxygen concentrations slowed biofilm growth rate, giving the biofilm more time to consolidate. In contrast, Applegate and Bryers (3) reported that oxygen-limited biofilms exhibited high EPS production, which in turn was associated with a high susceptibility to sloughing events. The conflicting conclusions of these researchers highlight the importance of studying not only specific EPS components but also a well-defined biofilm property, such as cohesiveness, as opposed to a property such as density, which is not necessarily related to the behavior of interest (sloughing in this case).

The fact that age did not affect biofilm cohesion in our study is not surprising, as results of aging are most likely accounted for by changes in polysaccharide concentration. In this study, we investigated a membrane-aerated biofilm in which counter-

gradients of oxygen and substrate exist (29, 30). Membrane-aerated biofilms are complex, with regions within the biofilm that are highly oxic and have low substrate concentrations, regions with high substrate concentrations but no DO, and conditions in between. As the biofilm grows, the nutrient diffusion limitation increases, resulting in a decrease of the growth rate in the active region. As a consequence, in a thick biofilm the base will be highly aerobic but the interface with the wastewater will be fully anaerobic. These changing growth conditions within the biofilm may influence EPS production and likely account for the gradients that we see in the polysaccharide concentration. This in turn affects the cohesive energy, resulting in surface layers of the biofilm having low polysaccharide concentrations and low levels of cohesive energy per unit volume. This is further illustrated by the biofilm grown without aeration. In the nonaerated biofilm, the polysaccharide concentration is very low, as is the cohesion.

Data reported in this paper should increase our ability to control biofilm behavior. For instance, our results suggest that to increase biofilm cohesion, high polysaccharide concentrations are needed and may be encouraged with aeration. Conditions for encouraging better biofilm cohesion could thus be achieved through design and use of reactor or biofilm supports, such as aerated-membrane supports. Such an approach could be applied for bioremediation of hazardous wastes and industrial production of enzymes, oils, and papers. In contrast, deprivation of oxygen may decrease polysaccharide production, which should weaken and slough unwanted biofilm. In addition, the development of biocides that specifically target polysaccharide linkages should result in weaker biofilms. Such approaches could have applications in the cleaning, food, and medical industries. This work should therefore stimulate more focused research on methodologies for enhancing or decreasing biofilm cohesion.

#### ACKNOWLEDGMENTS

This work was supported by the National Science Foundation under the GOALI Program (BES-0331953).

We also thank 3M Corporate (Saint Paul, MN) for providing materials and services.

#### REFERENCES

- Ahimou, F., M. J. Semmens, P. J. Novak, and G. Haugstad. Biofilm cohesiveness measurement using a novel atomic force microscopic methodology. *Appl. Environ. Microbiol.* **73**:2897–2904.
- Allison, D. G., B. Ruiz, C. San Jose, A. Jaspe, and P. Gilbert. 1998. Extracellular products as mediators of the formation and detachment of *Pseudomonas fluorescens* biofilms. *FEMS Microbiol. Lett.* **167**:179–184.
- Applegate, D. H., and J. D. Bryers. 1991. Effects of carbon and oxygen limitation and calcium concentration on biofilm removal processes. *Biotechnol. Bioeng.* **37**:17–25.
- Bayer, A. S., F. Eftekhar, J. Tu, C. C. Nast, and D. P. Speert. 1990. Oxygen-dependent up-regulation of mucoid exopolysaccharide (alginate) production in *Pseudomonas aeruginosa*. *Infect. Immun.* **58**:1344–1349.
- Bishop, P. L., T. C. Zhang, and Y. C. Fu. 1995. Effects of biofilm structure, microbial distributions and mass transport on biodegradation processes. *Water Sci. Technol.* **31**:143–152.
- Chen, X., and P. S. Stewart. 2002. Role of electrostatic interactions in cohesion of bacterial biofilms. *Appl. Microbiol. Biotechnol.* **59**:718–720.
- Cole, A. C., M. J. Semmens, and T. M. LaPara. 2004. Stratification of activity and bacterial community structure in biofilms grown on membranes transferring oxygen. *Appl. Environ. Microbiol.* **70**:1982–1989.
- Davies, D. G., A. M. Chakrabarty, and G. G. Geesey. 1993. Exopolysaccharide production in biofilms: substratum activation of alginate gene expression by *Pseudomonas aeruginosa*. *Appl. Environ. Microbiol.* **59**:1181–1186.
- Flemming, H. C., J. Wingender, C. Mayer, V. Korstgens, and W. Borchard. 2000. Cohesiveness in biofilm matrix polymers, p. 87–105. *In* D. Allison, P. Gilbert, H. M. Lappin-Scott, and M. Wilson (ed.), *Community structure and cooperation in biofilms*. SGM symposium series, vol. 59. Cambridge University Press, Cambridge, United Kingdom.
- Gaudy, A. F. 1962. Colorimetric determination of protein and carbohydrate. *Ind. Water Wastes* **7**:17–22.
- Gehrke, T., J. Telegdi, D. Thierry, and W. Sand. 1998. Importance of extracellular polymeric substances from *Thiobacillus ferrooxidans* for bioleaching. *Appl. Environ. Microbiol.* **64**:2743–2747.
- Grotenhuis, J. T., M. Smit, C. M. Plugge, Y. S. Xu, A. A. van Lammeren, A. J. Stams, and A. J. Zehnder. 1991. Bacteriological composition and structure of granular sludge adapted to different substrates. *Appl. Environ. Microbiol.* **57**:1942–1949.
- Higgins, M. J., and J. T. Novak. 1997. The effect of cations on the setting and dewatering of activated sludges: laboratory results. *Water Environ. Res.* **69**:215–224.
- Hughes, K. A., I. W. Sutherland, and M. V. Jones. 1998. Biofilm susceptibility to bacteriophage attack: the role of phage-borne polysaccharide depolymerase. *Microbiology* **144**:3039–3047.
- Jarman, T. R., L. Deavin, S. Slocombe, and R. C. Righelato. 1978. Investigation of the effect of environmental conditions on the rate of exopolysaccharide synthesis in *Azotobacter vinelandii*. *J. Gen. Microbiol.* **107**:59–64.
- Junkins, A. D., and M. P. Doyle. 1992. Demonstration of exopolysaccharide production by enterohemorrhagic *Escherichia coli*. *Curr. Microbiol.* **25**:9–17.
- Klapper, I., C. J. Rupp, R. Cargo, B. Purevdorj, and P. Stoodley. 2002. Viscoelastic fluid description of bacterial biofilm material properties. *Biotechnol. Bioeng.* **80**:289–296.
- Lapidou, C. S., and B. E. Rittmann. 2004. Modeling the development of biofilm density including active bacteria, inert biomass, and extracellular polymeric substances. *Water Res.* **38**:3349–3361.
- Lowry, O. H., N. J. Rosebrough, A. L. Farr, and R. J. Randall. 1951. Protein measurement with the folin phenol reagent. *J. Biol. Chem.* **193**:265–275.
- Mao, Y., M. P. Doyle, and J. Chen. 2001. Insertion mutagenesis of *wca* reduces acid and heat tolerance of enterohemorrhagic *Escherichia coli* O157:H7. *J. Bacteriol.* **183**:3811–3815.
- Mayer, C., R. Moritz, C. Kirschner, W. Borchard, R. Maibaum, J. Wingender, and H. C. Flemming. 1999. The role of intermolecular interactions: studies on model systems for bacterial biofilms. *Int. J. Biol. Macromol.* **26**:3–16.
- Mian, F. A., R. T. Jarman, and R. C. Righelato. 1978. Biosynthesis of exopolysaccharide by *Pseudomonas aeruginosa*. *J. Bacteriol.* **134**:418–422.
- Ohashi, A., and H. Harada. 1996. A novel concept for evaluation of biofilm adhesion strength by applying tensile force and shear force. *Water Sci. Technol.* **34**:201–211.
- Ohashi, A., T. Koyama, K. Sytsubo, and H. Harada. 1999. A novel method for evaluation of biofilm tensile strength resisting erosion. *Water Sci. Technol.* **39**:261–268.
- Ophir, T., and D. L. Gutnick. 1994. A role for exopolysaccharide in the protection of microorganisms from desiccation. *Appl. Environ. Microbiol.* **60**:740–745.
- Picioreanu, C., M. C. M. van Loosdrecht, and J. J. Heijnen. 1999. Discrete-differential modelling of biofilm structure. *Water Sci. Technol.* **39**:115–122.
- Raunkjær, K., T. Hvitved-Jacobsen, and P. H. Nielsen. 1994. Measurement of pools of protein, carbohydrate and lipid in domestic wastewater. *Water Res.* **28**:251–262.
- Ryu, J. H., and L. R. Beuchat. 2004. Factors affecting production of extracellular carbohydrate complexes by *Escherichia coli* O157:H7. *Int. J. Food Microbiol.* **95**:189–204.
- Semmens, M. J., and N. J. Essila. 2001. Modeling biofilms on gas-permeable supports: flux limitations. *J. Environ. Eng.* **127**:126–133.
- Shanahan, J. W., and M. J. Semmens. 2004. Multipopulation model of membrane-aerated biofilms. *Environ. Sci. Technol.* **38**:3176–3183.
- Shanahan, J. W., and M. J. Semmens. 2006. Influence of a nitrifying biofilm on local fluxes across a micro-porous flat-sheet membrane. *J. Membr. Sci.* **277**:65–74.
- Tay, J. H., Q. S. Liu, and Y. Liu. 2001. The role of cellular polysaccharides in the formation and stability of aerobic granules. *Letts. Appl. Microbiol.* **33**:222–226.
- Tijhuis, L., M. C. M. van Loosdrecht, and J. J. Heijnen. 1995. Dynamics of biofilm detachment in biofilm airlift suspension reactors. *Biotechnol. Bioeng.* **45**:481–487.
- Weiner, R., S. Langille, and E. Quintero. 1995. Structure, function and immunoreactivity of bacterial exopolysaccharides. *J. Ind. Microbiol.* **15**:339–346.
- Xavier, J. B., C. Picioreanu, S. A. Rani, M. C. M. van Loosdrecht, and P. S. Stewart. 2005. Biofilm-control strategies based on enzymic disruption of the extracellular polymeric substance matrix—a modeling study. *Microbiology* **151**:3817–3832.
- Zhang, T. C., and P. L. Bishop. 1994. Structure, activity and composition of biofilms. *Water Sci. Technol.* **29**:335–344.